運輸省港湾技術研究所

# 港湾技術研究所報告

REPORT OF
THE PORT AND HARBOUR RESEARCH INSTITUTE
MINISTRY OF TRANSPORT

VOL. 22 NO. 3 SEPT. 1983

NAGASE, YOKOSUKA, JAPAN

# 港湾技術研究所報告 (REPORT OF P.H.R.I.)

第22巻 第3号 (Vol. 22, No. 3), 1983年9月 (Sept. 1983)


## 目 次 (CONTENTS)


1. A Unified Nonlinearity Parameter of Water Waves
…… Yoshimi GODA…… 3

(水面波の非線型性パラメーターの統一的表示について……合田良実)

2. 無反射性造波方式の原理と推力制御式造波装置の特性
…… 谷本勝利・原中祐人・富田英治…… 31

(Principle and Performance of Non-reflective Wave Generator by Thrust Control
…… Katsutoshi TANIMOTO, Suketo HARANAKA and Eiji TOMIDA)

3. マイクロプロセッサ応用によるステップ式波高計の改良について
…… 佐々木 弘・高橋智晴…… 57

(Inprovement of step-type recording wave gauge with application of micro-processor
……Hiroshi SASAKI and Tomoharu TAKAHASHI)

4. 日本沿岸の波浪のスペクトル形について
…… 広瀬宗一・立花祐二・菅原一晃…… 83

(One-dimensional spectra of wind waves in coastal waters
…… Munekazu HIROSE, Yuji TACHIBANA and Kazuteru SUGAHARA)

5. 波力発電ケーソンの空気出力効率の解析
——波エネルギーに関する研究 第1報——
…… 小島朗史・合田良実・鈴村諭司…… 125

(Analysis of Efficiency of Pneumatic-type Wave Power Extractors Utilizing Caisson Breakwaters—A Study on Development of Wave Power 1st Report—
…… Roushi OJIMA, Yoshimi GODA and Satoshi SUZUMURA)

6. 海域における物質循環数値モデルの水質支配要因について
…… 堀江 毅・細川恭史…… 159

(Water-quality controlling factors in an eutrophication model
…… Takeshi HORIE and Yasushi HOSOKAWA)

7. 深層混合処理工法による壁状改良地盤の耐震性に関する実験的研究
…… 稲富隆昌・風間基樹・今村俊博…… 207

(An Experimental Study on the Earthquake Resistance of Wall Type Improved Ground by Deep Mixing Method
…… Takamasa INATOMI, Motoki KAZAMA and Toshihiro IMAMURA)

8. 川崎港海底トンネルでの地震応答観測と応答解析
…… 清宮　理・西澤英雄・横田　弘…… 253

(Field Observation and Response Analysis at Kawasaki Koh Submerged Tunnel
…… Osamu KIYOMIYA, Hideo NISHIZAWA and Hiroshi YOKOTA)

9. 港湾における空間設計手法の開発（第3報）
——入力方法の容易化と港湾計画への応用——
…… 奥山育英・梅山珠実・佐々木芳寛…… 301

(Development of Space Design of Port and Harbour (3rd Report)—Easy Input Methods and Application to Port Planning—
…… Yasuhide OKUYAMA, Tamami UMEYAMA and Yoshihiro SASAKI)

10. 港湾経済効果の計測手法（第2報）
——付加価値モデルの汎用化と原単位の整備——
…… 竹内良夫・米澤　朗・稲村　肇…… 325

(Development and Application of Synthetic Economic Evalution Model for Port Planning (2nd Report)—Value Added Model—
…… Yoshio TAKEUCHI, Akira YONEZAWA and Hajime INAMURA)

REPORT OF THE PORT AND
HARBOUR RESEARCH INSTITUTE
Vol. 22, No. 3 (Sept. 1983)

# 1. A Unified Nonlinearity Parameter of Water Waves

Yoshimi GODA*

## Synopsis

A new empirical parameter is proposed to describe the phenomena of wave nonlinearity. The parameter bridges the wave steepness in deep water and Ursell's parameter in very shallow water, spanning the full range of water waves.

Nonlinear properties of finite amplitude wave profiles are examined for the third order Stokes waves and the second order cnoidal waves. Relative crest elevations, the skewness and the ratio of wave height to root-mean-square surface elevation are expressed as unique functions of the new parameter. Laboratory data of regular waves in the range of relative water depth from 0.05 to 0.5 support the theoretical relationships between nonlinear properties and new parameter. Analysis of 128 wave records taken in coastal waters also supports these relationships.

Nonlinear components of wave spectrum are analyzed with the secondary interaction theory of Tick [1963] and Hamada [1965]. Growth of nonlinear spectral components in intermediate-depth to shallow water is governed by the new nonlinearity parameter. The mean wave period derived from spectrum, the spectral peakedness parameter, and the slope of wave spectrum in high frequency range all decrease as the value of nonlinearity parameter increases. The decreases are confirmed by the field data in coastal waters.

Thus, the newly proposed parameter is concluded to be effective in grasping the degree of wave nonlinearity and describing nonlinear properties of water waves.

* Director of Hydraulic Engineering Division

港湾技術研究所報告
第22巻 第3号 (1983. 9)

# 1. 水面波の非線型性パラメーターの統一的表示について

合 田 良 実*

## 要 旨

波浪の非線型現象を記述する新しい経験的パラメーターが提案された。このパラメーターは，深海波に対する波形勾配と長波に対するアーセル数を連続し，水面波の全範囲を統一的に表示する。

理論波形として第3次近似ストークス波と第2次近似クノイド波を用い，相対波頂高，波形のひずみ度，波高と波形の rms 値との比などを計算したところ，これらは新パラメーターの関数として統一的に表示できた。この関数関係は，水深波長比 0.05～0.5 の範囲における規則波の実験データならびに沿岸域における波浪観測記録128例によって確認される。

波浪スペクトルの非線型成分は Tick [1963] と浜田 [1965] の 2 次干渉理論によって解析されるが，浅海表面波から長波領域における非線型スペクトル成分の発達は，新しい非線型性パラメーターの値に支配される。スペクトルから計算される平均波周期，スペクトルの尖鋭度パラメーター，高周波側の勾配などはすべて非線型性パラメーターの増加につれて減少する。このことは沿岸域の波浪データによって確認される。

このように，新しく提案されたパラメーターは，波浪の非線型性の度合いを把握し，非線型現象を記述するのに有効であると考えられる。

* 水工部長

## CONTENTS


**Synopsis** ..... 3

**1. Introduction** ..... 7

**2. Proposal of New Nonlinearity Parameter** ..... 8

**3. Nonlinear Behaviours of Wave Profiles** ..... 8

3.1 Theoretical Profiles of Finite Amplitude Waves ..... 8

3.2 Profiles of Regular Waves in Laboratory ..... 12

3.3 Profiles of Sea Waves in Coastal Area ..... 15

**4. Nonlinear Behaviours of Wave Spectra** ..... 17

4.1 Nonlinear Interaction of Wave Spectrum ..... 17

4.2 Change of Spectral Parameters by Nonlinearity Effects ..... 20

**5. Discussions** ..... 25

**6. Conclusions** ..... 26

**References** ..... 27

**Appendix: List of Symbols** ..... 29

## 1. Introduction

Random nature of ocean waves is mostly described with the linear spectral model, and many engineering problems related to offshore and coastal structures are solved by employing the concept of directional wave spectra. A recent speciality conference entitled "Directional Wave Spectra Applications" [*Wiegel* 1982] as well as another international symposium of "Wave and Wind Directionality" [*ARAE* 1982] signify wide acceptance of directional spectra by scientists and engineers.

Waves in the sea, however, do exhibit some nonlinear properties. A departure of surface elevation from the Gaussian distribution with positive skewness is an example. Phase velocities of high frequency component waves not satisfying the linear dispersion relation is another example. Breaking of waves is a spectacular example of nonlinear behaviour of water waves.

The study of nonlinear water waves dates back to *Stokes* [1847], who showed a solution of finite amplitude waves in serial form. The kinematics of finite amplitude waves of permanent form have been extensively studied in the past three decades, owing to the acute need for reliable design formulae for offshore structures. Various theories of water waves are employed in these studies depending on the relative depth of water, and no single parameter has been found capable of describing the wave nonlinearity in the full range from deep to shallow water.

The linear wave spectral model is recently challenged by nonlinear wave models, which try to explain random wind waves as a sequence of groups of Stokes waves with envelope solitons [*e.g., Lake and Yuen* 1978 and *Mollo-Christensen and Ramamonjiarisoa* 1978]. These models have been stimulated by the phenomenon of regular wave train disintegrating into a series of group waves in the deep water. *Benjamin and Feir* [1967] are the first in noticing it, and *Merville* [1982] as well as *Su* [1982] present recent experimental verifications.

The applicability of these nonlinear wave models to ocean waves is uncertain at this stage. Extension of nonlinear models to the region of intermediate-depth to shallow water is neither foreseenable. From the engineering point of view, the linear spectral model serves well for the practical applications. Nonetheless we need to clarify the extent of wave nonlinearity in the sea so that we can solve engineering problems with much more confidence and accuracy.

One of the difficulties in the studies of wave nonlinearity is the lack of appropriate parameter to describe the degree of nonlinearity. Though the wave steepness is a good parameter in the deepwater region, its capacity decreases in the region of intermediate-depth to shallow water as there arises the necessity to incorporate the effect of water depth relative to wavelength. The present report is to propose a new single parameter which is capable of describing the nonlinearity of water waves from deep water to shallow water. It is admitted that the new parameter is an emprical one rather than a theoretical one, but it serves for the purpose of grasping the degree of wave nonlinearity and describing many nonlinear wave properties. After introducing it in Chapter 2, its capability in describing nonlinearity of wave profiles is discussed in Chapter 3 with the data of regular waves in laboratory and random waves observed in coastal water. Chapter 4 presents the computation of secondary interactions among linear spectral components and discusses the changes of spectral parameters by nonlinearity effects with the coastal wave data.

## 2. Proposal of New Nonlinearity Parameter

The parameter which represents the wave nonlinearity effects in deep water is the wave steepness, or a measure of the slope of surface elevation. The commonest representation is the ratio of wave height to wavelength, $H/L$*, although the parameter of $ak$, where $a$ denotes the wave amplitude and $k$ the wave number of $2\pi/L$, is employed in the derivation of finite amplitude wave theories as done by *Longuet-Higgins* [1975]. For ocean waves, *Huang and Long* [1980] employed the root-mean-square value of surface elevation $\eta_{rms}$ as the magnitude of height and the wavelength $L_p$ corresponding to the spectral peak frequency to define the significant slope of $\xi=\eta_{rms}/L_p$. However, the wave steepness most familiar with coastal engineers is the ratio of significant wave height $H_{1/3}$ to the wavelength corresponding to the significant wave period $T_{1/3}$, *i.e.*, $H_{1/3}/L_{1/3}$.

In the region of shallow water waves, *Ursell* [1957] has presented a nondimensional parameter of $\eta L^2/h^3$, where $\eta$ denotes the surface elevation above the mean water level and $h$ the water depth. This is called Ursell's parameter and has been shown to govern the transformation of water waves in shallow water. *Shuto* [1974], for example, has demonstrated that the nonlinear shoaling of water waves is predicted as the function of a Ursell's paremeter.

Thus, we have the parameter of $H/L$ in the one extreme and that of $HL^2/h^3$ in the other extreme. A logical way to bridge the two extremes is to introduce the follow-in new parameter:

$$\Pi=(H/L_A)\coth^3 k_A h\,, \tag{1}$$

where,

$$\omega^2=(2\pi/T)^2=g k_A \tanh k_A h\,, \quad \text{and} \quad k_A=2\pi/L_A\,. \tag{2}$$

The subscript $A$ is used here to denote the quantity being calculated by Airy's theory or the small amplitude wave theory. The use of $L_A$ and $k_A$ in Eq. 1 is to avoid the ambiguity in wavelength which varies slightly with the wave steepness.

The new parameter $\Pi$ is easily shown to approach to $H/L_A$ in deep water and to $(2\pi)^{-3}HL_A^2/h^3$ in the extreme of $k_A h\to 0$. Therefore, $\Pi$ is the parameter smoothly connecting the wave steepness in deep water and Ursell's parameter in very shallow water. In the following chapters, we shall see how the parameter $\Pi$ can describe the nonlinear properties of water waves.

## 3. Nonlinear Behaviours of Wave Profiles

### 3.1 Theoretical Profiles of Finite Amplitude Waves

#### (1) Third Order Theory of Stokes Waves

It is well acknowledged that the Stokes waves provide good representation of finite amplitude waves in deep water to intermediate-depth water, while cnoidal waves are applicable to finite amplitude waves in shallow water to intermediate-depth water,

* Major symbols employed in this report are listed alphabetically in the Appendix with their definitions.

even though the boundary of applicability cannot be defined clearly. Therefore, the present report computes profiles of Stokes waves and cnoidal waves with some overlapping in the range of relative water depth as the basis of theoretical wave profiles.

Among several higher order solutions of Stokes waves, the following third order solution by *Goda and Abe* [1968] is employed here because of its concise forms of equations:

$$k\eta=\left[\varepsilon+\frac{1}{2}\varepsilon^3 b_{11}\right]\cos\theta+\varepsilon^2 b_{22}\cos 2\theta+\frac{1}{2}\varepsilon^3 b_{33}\cos 3\theta\,, \tag{3}$$

where

$$\theta=kx-\omega t\,, \tag{4}$$

$$\varepsilon=ka_0\,, \tag{5}$$

$$b_{11}=\frac{1}{8}(3\coth^4 kh+8\coth^2 kh-9)\,, \tag{6}$$

$$b_{22}=\frac{1}{4}(3\coth^3 kh-\coth kh)\,, \tag{7}$$

$$b_{33}=\frac{3}{32}(9\coth^6 kh-3\coth^4 kh+3\coth^2 kh-1)\,. \tag{8}$$

The wave height $H$ is given as

$$kH=2\varepsilon+\varepsilon^3(b_{11}+b_{33})\,. \tag{9}$$

The dispersion relation is

$$\omega^2=gk\tanh kh\left[1+\frac{1}{2}\varepsilon^2 C_1\right]^2\,, \tag{10}$$

where

$$C_1=\frac{1}{8}(9\coth^4 kh-10\coth^2 kh+9)\,. \tag{11}$$

The above relation can be rewritten in terms of the small amplitude wave number $k_A$ of Eq. 2 as in the following:

$$k_A h\tanh k_A h=kh\tanh kh\left[1+\frac{1}{2}\varepsilon^2 C_1\right]^2\,. \tag{12}$$

The above solution has a form different from that by *Skjelbreia and Hendrickson* [1960], but it can be shown that they agree each other to the third order of approximation by adjusting the difference in the relation between $kH$ and $\varepsilon$ [*Goda and Abe* 1968].

Calculation of wave profiles with the above solution is done for a given set of the wave steepness $H/L_A$ and the relative water depth $h/L_A$, by numerically solving Eqs. 9 and 12 for $kh$ and $\varepsilon$. For this purpose, the value of $\varepsilon$ is sought for by the bisection algorithm with the initial range of 0 to $\pi H/L_A$. The relative water depth $h/L_A$ employed in the calculation varied from 0.05 to 1.0.

**(2) Second Order Theory of Cnoidal Waves**

The present report employs the second order approximation of cnoidal waves

by *Laitone* [1960]. The formulae of wave profiles and others have been rewritten by *Iwagaki* [1963] as in the following:

$$\frac{\eta}{H}=\mathrm{cn}^2\left(2K\frac{x}{L},\kappa\right)-\frac{3}{4}\frac{H}{h_t}\mathrm{cn}^2\left(2K\frac{x}{L},\kappa\right)\left[1-\mathrm{cn}^2\left(2K\frac{x}{L},\kappa\right)\right]-\frac{\eta_t}{H}, \tag{13}$$

$$\frac{\eta_t}{H}=\frac{1}{\kappa^2}\left(\frac{E}{K}-1+\kappa^2\right)+\frac{H}{h_t}\frac{1}{12\kappa^4}\left[(1-\kappa^2)(8-3\kappa^2)-(8-7\kappa^2)\frac{E}{K}\right], \tag{14}$$

$$\frac{C}{\sqrt{gh}}=\left(\frac{h_t}{h}\right)^{1/2}\left\{1+\frac{H}{h_t}\frac{1}{\kappa^2}\left(\frac{1}{2}-\frac{E}{K}\right)+\left(\frac{H}{h_t}\right)^2\frac{1}{\kappa^4}\left[\frac{E}{K}\left(\frac{E}{K}+\frac{3}{4}\kappa^2-1\right)-\left(\frac{\kappa^4+14\kappa^2-9}{40}\right)\right]\right\}, \tag{15}$$

$$\frac{L}{h}=\frac{4\kappa K}{\sqrt{3}}\left(\frac{h_t}{h}\right)^{3/2}\left(\frac{h}{H}\right)^{1/2}\Big/\left[1-\frac{7\kappa^2-2}{8\kappa^2}\frac{H}{h_t}\right], \tag{16}$$

where cn is the Jacobian elliptic function associated with cosine, $\kappa$ denotes the modulus of elliptic function, $K$ and $E$ are the complete elliptic integrals of the first and second kind respectively, $h_t$ is the water depth below the wave trough, and $C$ denotes the wave celerity.

Cnoidal wave profiles are calculated for a given set of the modulus $\kappa$ and the relative wave height $H/h$ as in the following procedure. First, the water depth below troughs is estimated with the first approximation as

$$\frac{h}{h_t}=1+\frac{\eta_t}{h_t}\fallingdotseq 1+\frac{H}{h}\frac{1}{\kappa^2}\left[\frac{E}{K}-1+\kappa^2\right]. \tag{17}$$

With the first estimate of $h_t$, wave profiles are calculated, but the mean of $\eta$ usually remains at a nonzero value because of the approximation error in the estimate of $h_t$. This difference in the mean water level is simply adjusted by shifting the mean level of $\eta$. Therefore, the second term in the right-hand side of Eq. 14, which has been pointed out as incorrect by *Horikawa and Nishimura* [1976], is not calculated in the present report. Then Eqs. 15 and 16 are calculated to yield the nondimensional wave period of

$$T\sqrt{\frac{g}{h}}=\frac{L}{h}\Big/\frac{C}{\sqrt{gh}}. \tag{18}$$

From this nonlinear wave period, the ratio of water depth to deepwater wavelength is easily derived and the relative water depth $h/L_A$ is recovered. The wave nonlinearity parameter $\Pi$ is then calculated with the information of $H/h$ and $h/L_A$ by Eq. 1. Calculation has been done for the range of $\kappa^2=0.5$ to $(1-10^{-9})$ and $H/h=0.01$, 0.1, 0.2 and 0.4.

### (3) Examples of Calculated Wave Profiles and Some Descriptive Parameters

Figure 1 shows the theoretical profiles of Stokes waves and cnoidal waves for the nonlinearity parameter $\Pi$ being 0.1 and 0.35. Both theories yield quite similar profiles with almost the same crest elevation, though the Stokes waves of third order approximation for $\Pi=0.35$ exhibit double humps at wave troughs. The appearance of such humps is an indication that the wave condition exceeds the limit of applicability of the theory and a higher order approximation becomes necessary.

From such wave profiles, the following parameters describing the characteristics of wave profiles are computed.

1) Ratio of wave crest elevation above the mean water level to the wave height, $\eta_c/H$,
2) Skewness of wave profile, $\sqrt{\beta_1}$,
3) Ratio of wave height to the root-mean-square value of surface elevation, $H/\eta_{rms}$.

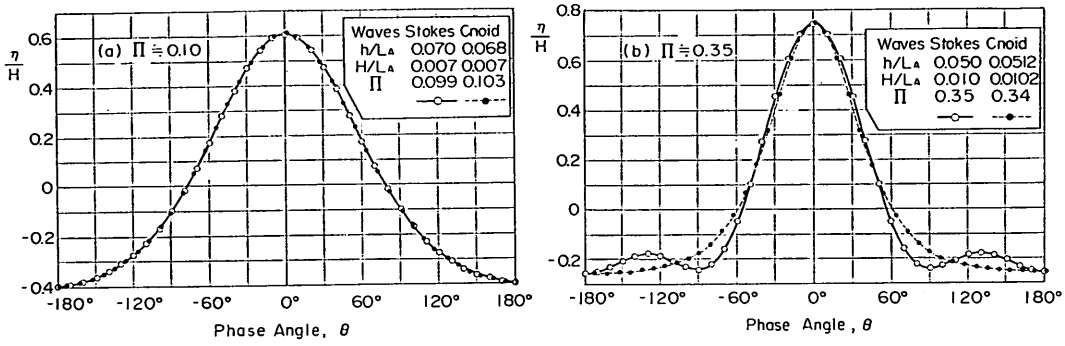


**Fig. 1** Profiles of Stokes Waves of Third Approximation and Cnoidal Waves of Second Approximation

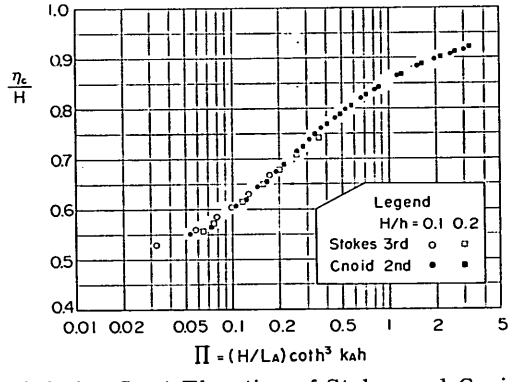


**Fig. 2** Relative Crest Elevation of Stokes and Cnoidal Waves in Terms of Nonlinearity Parameter

The result of the calculation of relative crest elevation is shown in Fig. 2. Such information of crest elevation is much sought in the design of offshore structures as it is the elevation to which wave actions extend. For the range of $H/h$ not exceeding 0.2, the theories of Stokes and conidal waves yield a consistant relationship between $\eta_c/H$ and $\Pi$. Strictly speaking, the relationship of $\eta_c/H$ versus $\Pi$ of the Stokes waves is slightly affected by the value of relative water depth $h/L_A$, and the relative crest elevation is better correlated with a parameter of $(H/L_A)$ $(3\coth^3 k_A h - \coth k_A h)/2$ than $\Pi$ as conceived from the coefficient of $b_{22}$ in Eq. 7. However, the effect of $h/L_A$ is of negligible magnitude from the practical point of view.

For the range of $H/h$ exceeding 0.2, calculated wave profiles show slightly lower crest elevation than the relation shown in Fig. 2. There is a possibility that the difference is due to the insufficiency in the accuracy of approximation, but its examination

will require the computation of higher order theories such as the stream function method by *Dean* [1965] and the numerical analysis by *Horikawa and Nishimura* [1976].

Figure 3 shows the skewness of Stokes and cnoidal waves as a function of the nonlinearity parameter $\Pi$. For the range of $\Pi \gtrsim 0.15$, the Stokes waves of third order approximation indicate smaller values of skewness than cnoidal waves of second order approximation, even though the relative crest elevations of both waves do not show marked difference. This is because the skewness is more sensitive to the shape of wave profile than the relative crest elevation, and a formation of humps at wave troughs such as shown in Fig. 1 (b) certainly decreases the value of skewness.

Next, the ratio of wave height to the root-mean-square value of surface elevation is plotted in Fig. 4. This ratio is examined here, because it is a quantity of interest in the analysis of sea waves in such a way whether the theoretical relation of $H_{1/3}=4\eta_{\mathrm{rms}}$ derived from the Rayleigh distribution does hold for sea waves or not. In fact, most of field data suggest a mean relation of $H_{1/3}=3.8\eta_{\mathrm{rms}}$ [e.g., *Goda* 1979], but coastal waves in relatively shallow water tend to support the theoretical relation of $H_{1/3}=4.0\eta_{\mathrm{rms}}$ [*Goda* 1974]. When *Longuet-Higgins* [1980] examined the distribution of heights of sea waves, he estimated the effect of wave nonlinearity in the direction to increase the ratio of $H_{1/3}/\eta_{\mathrm{rms}}$. As shown in Fig. 4, the ratio increases for regular waves too with the increase of wave nonlinearity expressed in terms of $\Pi$.

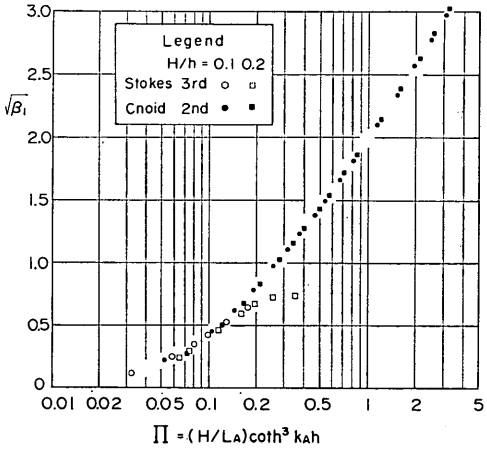


**Fig. 3** Skewness of Stokes and Cnoidal Waves in Terms of Nonlinearity Parameter

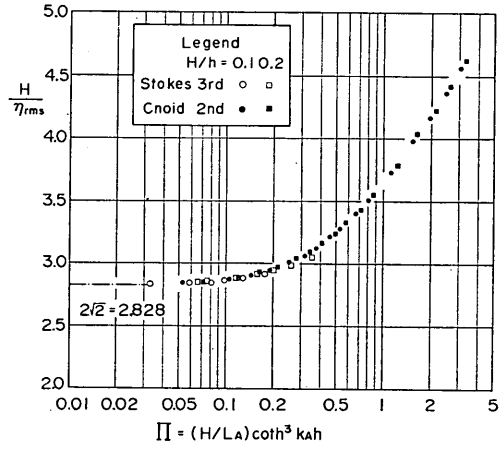


**Fig. 4** Rario of Wave Height to Root-Mean-Square Surface Elevation in Terms of Nonlinearity Parameter

The results of Figs. 2 to 4 indicate that the nonlinear properties of theoretical wave profiles are well described with the newly proposed nonlinearity parameter $\Pi$. At the same time, the applicability of the third order approximation of Stokes waves may be concluded as $\Pi=0.2$ or less on the basis of calculated wave profiles.

### 3.2 Profiles of Regular Waves in Laboratory

#### (1) Wave Data

A systematic data of wave profiles has been obtained by the author [1964] in the range of $h/L_A=0.05$ to 0.5. Experiments were carried out by increasing wave

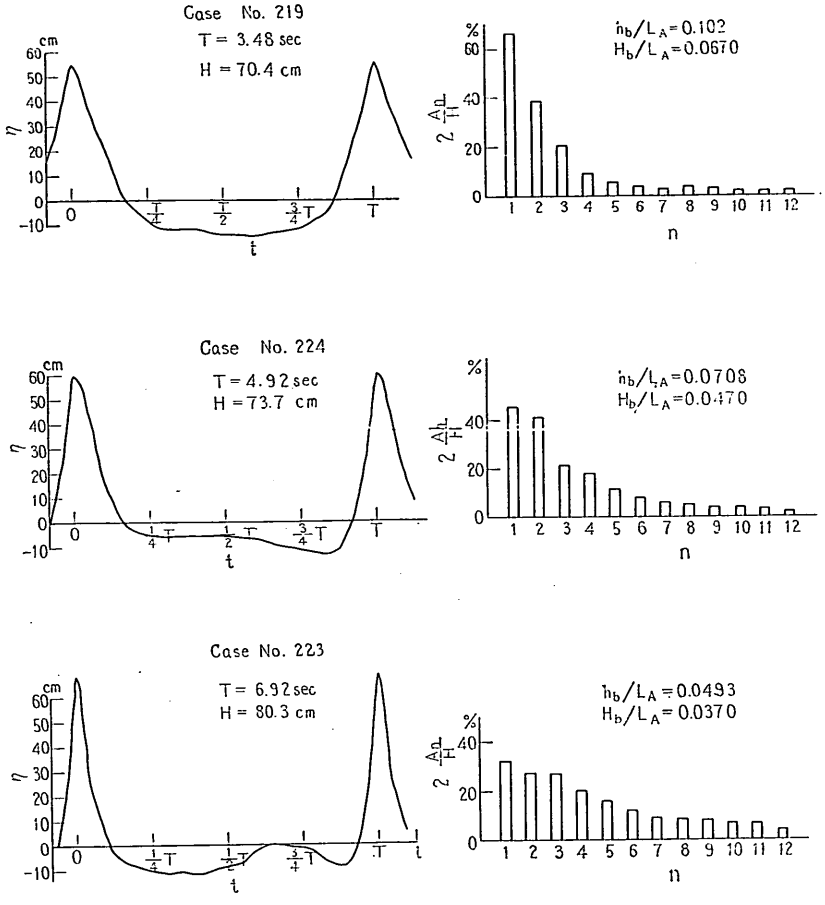


**Fig. 5** Examples of Time History of Breaking Waves and Relative Amplitudes of Fourier Components

heights gradually up to the breaking limit, while keeping the value of $h/L_A$ at a prescribed value by controlling the wave period. The data is characterized with large values of wave heights ranging up to 90 cm at the water depth of about 120 cm. Figure 5 has been taken from *Goda* [1964], showing three examples of the time histories of breaking wave profiles on a gently sloping bed; the right-hand side of Fig. 5 shows the relative magnitudes of Fourier components of wave profiles. The wave record of Case No. 223 exhibits a presence of secondary wave crest, which propagates with lesser celerity than the primary crest. Some of nonbreaking waves on a horizontal bed with the relative water depth of $h/L_A$=0.05 and 0.07 exhibited much enhanced secondary wave crests.

### (2) Nonlinear Properties of Laboratory Wave Profiles

Laboratory data of the relative crest elevation $\eta_c/H$ is shown in Fig. 6. The effect of the relative water depth $h/L_A$ on the relation between $\eta_c/H$ and $\Pi$ cannot be recognized as expected from the result of theoretical wave profiles, although the scatter of data hinders the examination of such effect even if there exists any. The departure

of laboratory data from the curve of Stokes and cnoidal waves in the range of $\Pi=0.2$ to 1.0 for $h/L_A=0.05$, 0.07, and 0.10 is considered as the effect of presence of secondary wave crests, because breaking waves with fewer secondary crests almost follow the curve of theoretical wave profiles. The result of Fig. 6 indicates that the relative crest elevation of theoretical profiles provides an upper envelope to laboratory data.

Figure 7 shows the ratio of $H/\eta_{rms}$ of laboratory data. The root-mean-square value $\eta_{rms}$ were recalculated from the original data which had been tabulated at 24 equi-spaced points per wave period. The theoretical wave profiles provide a lower envelope in this case. The difference between laboratory data and theoretical profiles is considered mainly due to the insufficiency in the accuracy of wave theory. According to *Longuet-Higgins* [1975], the variance of surface elevation of deepwater waves is approximated as

$$\eta_{rms}^2=\frac{1}{8}H^2\left\{1-\frac{1}{2}\left(\frac{\pi H}{L}\right)^2-\frac{19}{12}\left(\frac{\pi H}{L}\right)^4-\frac{3077}{720}\left(\frac{\pi H}{L}\right)^6-\cdots\right\}. \tag{19}$$

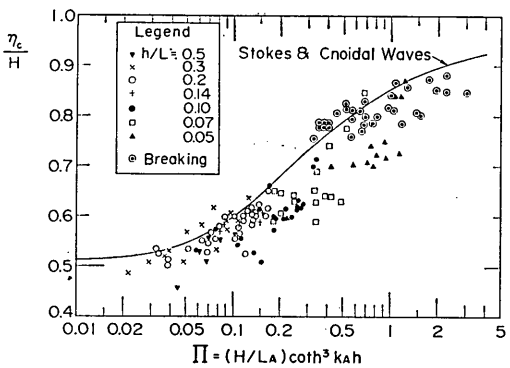


**Fig. 6** Laboratory Data of Relative Crest Elevation versus Wave Nonlinearity Parameter

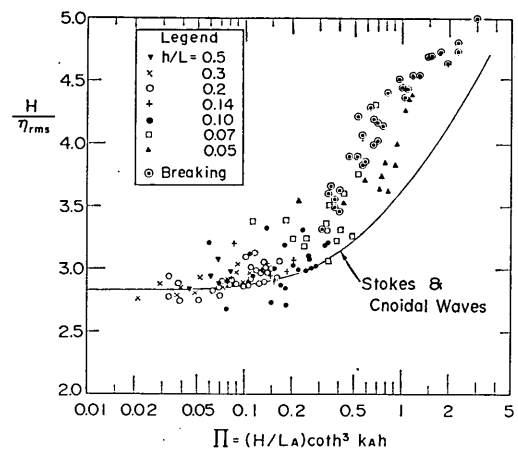


**Fig. 7** Laboratory Data of the Ratio of Wave Height to Root-Mean-Square Surface Elevation versus Wave Nonlinearity Parameter

On the other hand, the third order approximation of Stokes waves of Eqs. 3 to 9 yields for the deepwater waves:

$$\left.\begin{aligned} k^2\eta_{rms}^2&=\frac{1}{2}\varepsilon^2\left[1+\frac{1}{2}\varepsilon^2+\frac{5}{32}\varepsilon^4\right]+0(\varepsilon^6)\,,\\ \text{and}\qquad kH&=2\varepsilon\left[1+\frac{1}{2}\varepsilon^2\right]+0(\varepsilon^5)\,. \end{aligned}\right\} \tag{20}$$

This can be rewritten as

$$\eta_{rms}^2=\frac{1}{8}H^2\left\{1-\frac{1}{2}\left(\frac{\pi H}{L}\right)^2+\frac{19}{32}\left(\frac{\pi H}{L}\right)^4+0\left[\left(\frac{\pi H}{L}\right)^6\right]\right\}. \tag{21}$$

Clearly, Eq. 21 yields a larger value of $\eta_{rms}/H$ for a given value of $H/L$ than Eq. 19, and thus a smaller ratio of $H/\eta_{rms}$.

In any case, a clear relationship exists between the laboratory data of $H/\eta_{rms}$ and $\Pi$, which verifies the validity of wave nonlinearity parameter $\Pi$.

### 3.3 Profiles of Sea Waves in Coastal Area

#### (1) Wave Data

The field data of coastal waves examined herein are those reported by the author previously [*Goda and Nagai* 1974, *Goda* 1974 and 1983]. Principal data of wave observations are listed in Table 1. The stations of Rumoi and Kanazawa are located at the Japan Sea Coast of Hokkaido and Honshu, respectively, the stations of Tomakomai and Yamase-domari are positioned at the southwestern shore of Hokkaido, Japan, facing the Pacific Ocean, and Caldera Port is at the Pacific Coast of Costa Rica, Central America. The total number of wave records is 128.

**Table 1** Description of Wave Data

| Port | Location | Nos. | Depth (m) | $H_{1/3}$ (m) | $T_{1/3}$ (s) | $h/L_A$ | Type of Sensors |
|---|---|---|---|---|---|---|---|
| Rumoi | 43°55′N 141°36′E | 44 | 12~13 | 2.2~7.0 | 6~12 | 0.09~0.23 | Step-resis. |
| Tomakomai A | 42°37′N 141°36′E | 8 | 10~11 | 2.9~5.8 | 8~11 | 0.10~0.16 | Step-resis. |
| B | 42°36′N 141°36′E | 3 | 13~14 | 2.4~2.6 | 7 | 0.20~0.21 | Step-resis. |
| C | 42°36′N 141°36′E | 2 | 20~21 | 2.6~2.8 | 7~8 | 0.26~0.31 | Acoustic |
| Yamase-domari | 41°47′N 141°08′E | 9 | 12~13 | 1.9~6.2 | 8~14 | 0.09~0.17 | Step-resis. |
| Kanazawa | 36°38′N 136°35′E | 13 | 20~21 | 1.0~6.8 | 5~12 | 0.13~0.59 | Acoustic |
| Caldera | 10°25′N 84°43′W | 49 | 15~18 | 1.5~3.6 | 14~18 | 0.08~0.10 | Acoustic |

Wave sensors are the step-resistance gauges and the acoustic type of inverted echo sounders. The data length was mostly 1000 to 1200 seconds, but the data of Kanazawa Port were about 600 seconds long, while many of Caldera Port were about 1800 seconds long. Each wave record was analyzed by the zero-upcrossing method to yield $H_{1/3}$, $T_{1/3}$, and other representative wave heights and periods. In addition, the variance spectrum of each wave record was calculated. Spectral analysis was made by the Blackman-Tukey method for the data of Rumoi, Tomakomai, Yamase-domari, and Kanazawa with the frequency resolution of 0.01 to 0.02 Hz, while the data of Caldera Port was analyzed by the fast Fourier transform method with the frequency resolution of 0.0039 Hz. Almost all wave spectra had single peaks and the frequencies at spectral peaks were determined by fitting smooth curves around the peaks.

#### (2) Nonlinear Properties of Field Wave Profiles

Figure 8 shows the ratio of the highest surface elevation above the mean water level to the highest wave height in a wave record; $\eta_{max}$ and $H_{max}$ do not necessarily belong to the same wave. The wave nonlinearity parameter $\Pi_{max}$ in this figure is

calculated with the highest wave height $H_{max}$ and the small amplitude wavelength $L_A$ corresponding to the significant wave period $T_{1/3}$. The use of significant wave period to calculate $L_A$ is to avoid the introduction of large fluctuations of highest wave period $T_{max}$ into $\Pi_{max}$. The field data of $\eta_{max}/H_{max}$ approximately follows the curve of theoretical wave profiles of Stokes and cnoidal waves presented in Fig. 2. The large scatter of data is a phenomenon inherent to the data of highest wave in a wave record because of its low statistical stability.

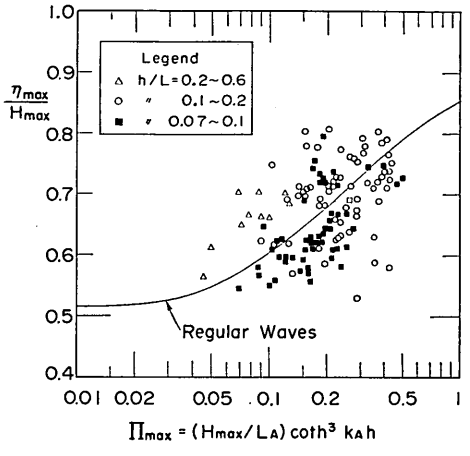


**Fig. 8** Coastal Wave Data of Relative Crest Elevation versus Wave Nonlinearity Parameter Defined with Highest Wave

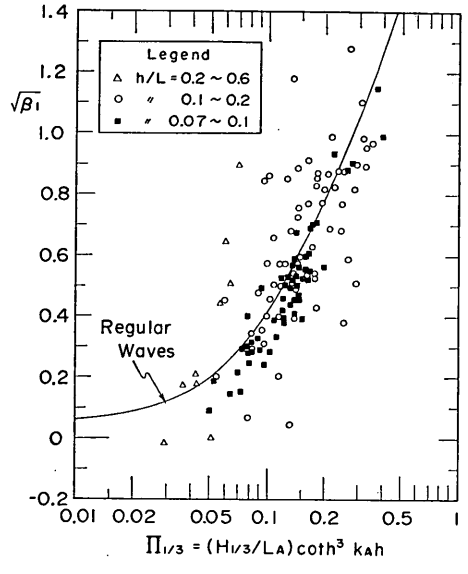


**Fig. 9** Coastal Wave Data of Skewness of Surface Elevation versus Wave Nonlinearity Parameter Defined with Significant Wave

The skewness $\sqrt{\beta_1}$ of field data is plotted in Fig. 9 against the wave nonlinearity parameter of $\Pi_{1/3}$ defined with the height and period of significant wave. The scatter of data is less than that of $\eta_{max}/H_{max}$, and the skewness of field waves on the average is in agreement with the data of theoretical wave profiles. The skewness of theoretical finite amplitude waves can be approximated with the relation of $\sqrt{\beta_1} \fallingdotseq 4.2\Pi$ for the range of $\Pi < 0.15$. This linearity between the skewness and the steepness of wind waves in deep water has been observed by *Huang and Long* [1980]. They proposed a relation of $\sqrt{\beta_1} = 8\pi\eta_{rms}/L_p$, where $L_p$ denotes the wavelength corresponding to the frequency at spectral peak. This relation is also supported by remote sensing data of *McClain et al.* [1982]. By converting the root-mean-square surface elevation into the significant wave height with the relation of $H_{1/3} \fallingdotseq 4\eta_{rms}$, their formula becomes $\sqrt{\beta_1} \fallingdotseq 2\pi H_{1/3}/L_p$, which is about 50% greater than the present relation of $\sqrt{\beta_1} \fallingdotseq 4.2H_{1/3}/L_A$. The cause of discrepancy is not certain. A speculation is such that the presence of wind shear in deep water may produce more nonlinear wave profiles than those of finite amplitude waves of permanent forms.

Furthermore, the ratio of $H_{1/3}/\eta_{rms}$ is presented in Fig. 10 against the wave nonlinearity parameter of $\Pi_{1/3}$. The theoretical curve has been obtained by numerically evaluating the potential energy of individual waves under the assumption of the Ray-

leigh distribution law for wave heights by making use of the curve shown in Fig. 4. It is based on the same concept employed by *Longuet-Higgins* [1980], though he has obtained the variation of potential energy in a form of serial approximation. As discussed earlier, the field data at a low value of $\Pi_{1/3}$ takes the value of $H_{1/3}/\eta_{rms}$ less than 4.0; a commonly reported mean value of 3.8 fits to the present data in the range of $\Pi_{1/3} < 0.1$. As the wave nonlinearity parameter increases, the ratio of $H_{1/3}/\eta_{rms}$ begins to increase. The rate of increase seems greater than the trend of theoretical curve. This difference is in the same direction with the data of laboratory wave profiles presented in Fig. 7.

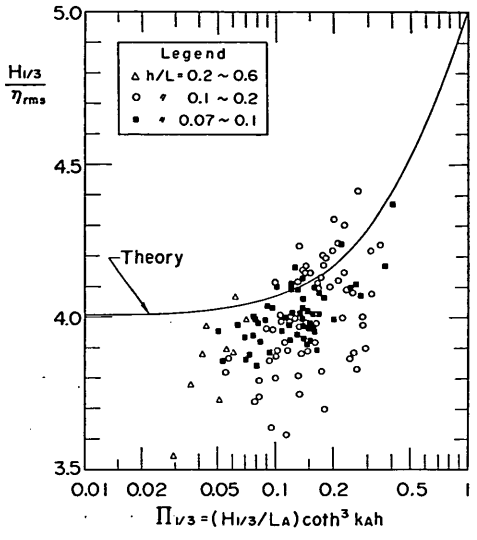


**Fig. 10** Coastal Wave Data of the Ratio of Significant Wave Height to Root-Mean-Square Surface Elevation versus Wave Nonlinearity Parameter Defined with Significant Wave

The results of Figs. 8 to 10 all indicate that the nonlinear properties of field wave data can be described with the newly proposed nonlinearity parameter. Though the data have been classified with three ranks of relative water depth, its effects are not observable in Figs. 8 to 10, partly because of large scatters of data which are unavoidable in any analysis of field wave data. Thus the functional representation of the effects of $h/L_A$ on $\Pi$ is considered acceptable at the present level of statistical reliability.

## 4. Nonlinear Behaviours of Wave Spectra

### 4.1 Nonlinear Interaction of Wave Spectrum

In the previous report [*Goda* 1983], the author presented an example of nonlinear components of observed wave spectrum by using the theory of *Tick* [1963] and *Hamada* [1965]. The theory predicts the density of nonlinear spectral components as the result of secondary interactions between linear spectral components. The second order sectrum denoted by $S^{(2)}(f)$ is given by

$$S^{(2)}(f_1) = \int_{-\infty}^{\infty} K(\omega, \omega_1) S^{(1)}(f_1 - f) S^{(1)}(f)\, df\,, \tag{22}$$

in which

$$K(\omega, \omega_1) = \frac{1}{4}\left\{\frac{gkk'}{\omega(\omega_1-\omega)} + \frac{\omega(\omega_1-\omega)}{g} - \frac{\omega_1^2}{g} + \frac{\omega_1^2\left[\frac{g(\omega_1-\omega)k^2+g\omega k'^2}{\omega(\omega_1-\omega)\omega_1} + \frac{2gkk'}{\omega(\omega_1-\omega)} + \frac{\omega(\omega_1-\omega)}{g} - \frac{\omega_1^2}{g}\right]}{g|k+k'|\tanh|k+k'|h - \omega_1^2}\right\}^2, \tag{23}$$

$$\omega^2=gk\tanh kh\ ,\qquad (\omega_1-\omega)^2=gk'\tanh k'h\ , \tag{24}$$

where $S^{(1)}(f)$ represents the linear spectrum.

The observed spectrum which is a sum of linear and nonlinear components can be decomposed by an iteration technique employed by *Masuda et al.* [1979]. Figure 11 shows two examples of spectral resolution of linear and nonlinear components for the observed spectra at Caldera Port. These are addition to the example introduced in the previous report, and the same procedure of computation has been employed. The observed spectra are the arithematic means of five or six consecutive spectra of 30 minutes long records, because the nature of long-travelled swell made it appropriate to assume quasi-stationarity for the period of a few hours.

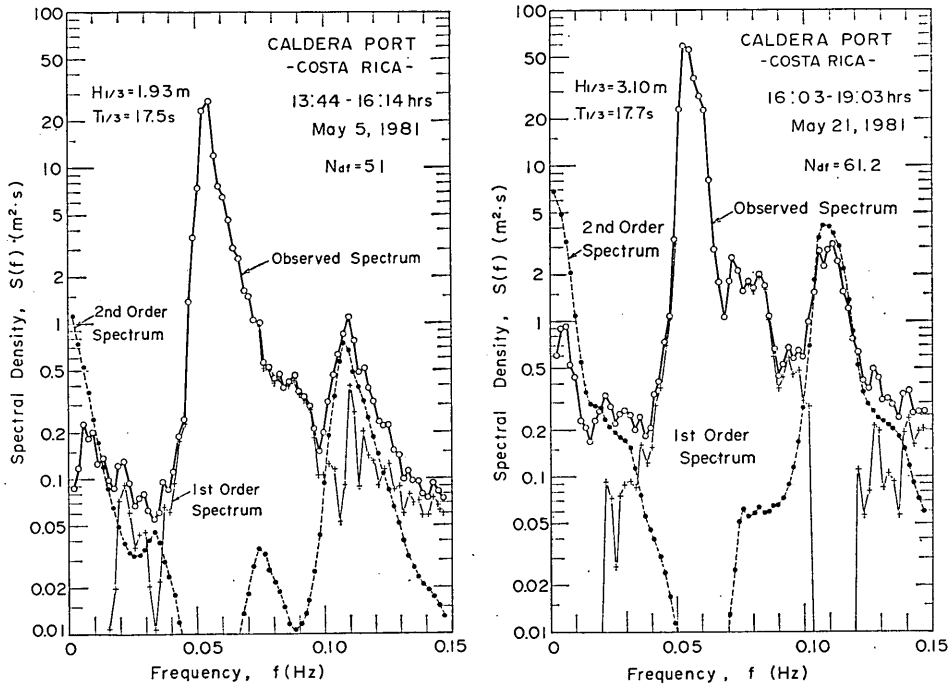


(a) Wave Data of May 5, 1981 (b) Wave Data of May 21, 1981

**Fig. 11** Examples of Resolution of Observed Spectra into Linear and Nonlinear Components

The examples shown in Fig. 11 indicate that the secondary spectral peaks located at the frequencies of twice the main peak frequency are the product of secondary interactions and that humps in the range of frequency below 0.03 Hz are also due to the same cause. Though some portions of second order spectra have the magnitude in excess of the observed spectra, probably owing to the inadequacy in the accuracy of theory, the secondary interaction theory is quite useful in predicting the formation of nonlinear spectral components. Thus, a calculation was made to investigate how the spectral shape varies as waves propagate from deep water to shallow water by the process of secondary nonlinear interactions.

Figure 12 shows an example of spectral deformation from deep water to the

water depth of 9.4 m for waves with the significant height of $H_{1/3}=6$ m and the peak period of $T_p=10$ s. The spectral function employed is a JONSWAP type of the following with $\gamma=3.3$:

$$S(f)=\alpha_* H_{1/3}^2 T_p^{-4} f^{-5} \exp\left[-\frac{5}{4}(T_p f)^{-4}\right]\gamma^{\exp[-(T_p f-1)^2/2\sigma^2]}, \tag{25}$$

where

$$\alpha_*=\frac{0.0624}{0.230+0.0336\gamma-0.185(1.9+\gamma)^{-1}}, \tag{26}$$

$$\sigma=\begin{cases} 0.07 & \text{for } f\leq f_p, \\ 0.09 & \text{for } f>f_p. \end{cases} \tag{27}$$

The formulation of coefficient $\alpha_*$ has been made by the author [1977] based on the numerical integration of JONSWAP-type spectra for the range of $\gamma=1$ to 10. The effect of wave shoaling is excluded in the computation of Fig. 12 in order to focus our attention upon the process of nonlinear interaction.

The result shown in Fig. 12 demonstrates a rapid growth of the secondary spectral peak and low-frequency hump as the water depth decreases below 10 m or so in this case. In the physical situation, breaking of larger waves in a wave train will begin in the water of some 15 m deep and wave breaking will be quite intensive at the water depth of 9.4 m. Thus, actual spectral shapes in the shallow water region will be different from those shown in Fig. 12. Presence of tertiary and higher order interactions modifies the spectral shape too. Nevertheless the process of nonlinear interaction of spectral components is an important matter to be paid attention in the analysis of wave records.

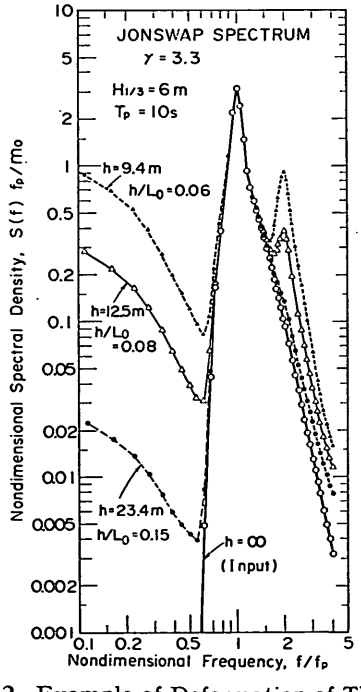


**Fig. 12** Example of Deformation of Theoretical Wave Spectrum in Intermediate-Depth Water as the Result of Nonlinear Wave Interactions

One feature of nonlinear deformation of wave spectra is an apparent increase of the area under the spectral curve, which is equal to the variance of surface elevation. Figure 13 presents the result of computation for the apparent increase of nominal wave height which is estimated with the square-root of the zero-th spectral moment. The JONSWAP-type spectra with $\gamma=1$ and 10 were employed for the significant wave height ranging from 1 to 10 m at the peak period of 10 s. The apparent increase of nominal wave height given by $\sqrt{(m_0)_2/(m_0)_1}$ is almost governed by the newly defined wave nonlinearity parameter of $\Pi_{1/3}$.

### 4.2 Change of Spectral Parameters by Nonlinearity Effects

#### (1) Mean Zero-upcrossing Wave Period

The change of spectral shapes due to nonlinear wave interaction affects various spectral-dependent parameters. The first of them is the mean zero-upcrossing wave period, which is often estimated with the following formula after *Rice* [1944]:

$$T_{0,2}=\sqrt{m_0/m_2}\,, \tag{28}$$

where

$$m_n=\int_0^\infty f^n S(f)\,df\,. \tag{29}$$

Appearance of secondary and higher order spectral peaks causes apparent increase of the second spectral moment $m_2$ and thus apparent decrease of the mean zero-upcrossing period. Figure 14 shows the result of computation for the ratio of $T_{0,2}/T_p$ with the JONSWAP-type spectra of $\gamma=1$ and 10 in the range of $H_{1/3}=1$ to 10 m at $T_p=10$ s. Though the decrease of $T_{0,2}/T_p$ is somewhat affected by the absolute magnitude of wave height, the variation of $T_{0,2}/T_p$ due to wave nonlinearity effects is well described as the function of the parameter $\Pi_{1/3}$.

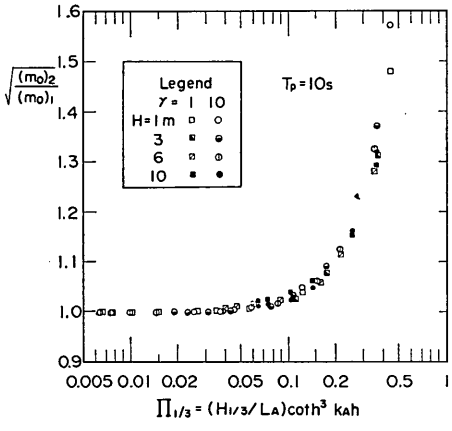


**Fig. 13** Apparent Increase of the Zero-th Moment of JONSWAP-type Spectrum in Terms of Wave Nonlinearity Parameter

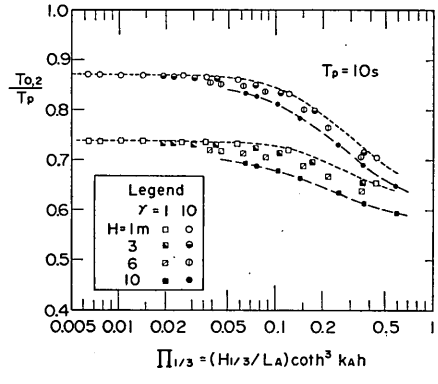


**Fig. 14** Apparent Decrease of Mean Zero-Upcrossing Period for JONSWAP-type Spectrum in Terms of Wave Nonlinearity Parameter

Figure 15 presents the field data of coastal waves for $T_{0,2}/T_p$. The data marked with closed squares mostly belong to the swell observed at Caldera Port, thus having very sharp spectral peaks equivalent to $\gamma=8$ to 9. The data with closed squares below the line of $\gamma=1$ all belong to wind waves or young swells observed at coastal station around Japan; their spectral peaks are not sharp. The result of Fig. 15 confirms the decrease of the ratio of $T_{0,2}/T_p$ with the increase of wave nonlinearity parameter as well as the influence of spectral shape upon $T_{0,2}/T_p$. The field data as a whole exhibits more rapid decrease of mean zero-upcrossing period than the secondary interaction theory predicts. The difference is partly attributed to the tertiary and higher order

interactions of spectral components, which raise the spectral density level at higher frequency side and cause to increase the second moment of wave spectrum.

The apparent decrease of mean zero-upcrossing period also distorts the equivalence of the spectrally estimated mean period of $T_{0,2}$ and the individually counted mean period of $\bar{T}_z$. As reviewed by the author [1979], there are several reports that $T_{0,2}$ is shorter than $\bar{T}_z$ although some other reports support the quasi-equivalency. Figure 16 compares the field data with the theoretical prediction of the ratio of $T_{0,2}/\bar{T}_z$; the mean period calculated with the original linear spectrum is presumed to represent the true period equal to $\bar{T}_z$. The difference in spectral shape yields only a slight difference in the ratio of $T_{0,2}/\bar{T}_z$. The tendency of the decrease of $T_{0,2}/\bar{T}_z$ with the increase of wave nonlinearity parameter is common in both the field data and the spectral calculation, but the field data indicate much greater decrease than the theory. The difference is again attributable to the tertiary and higher order interactions of spectral components, though detailed analysis is not attempted at this stage.

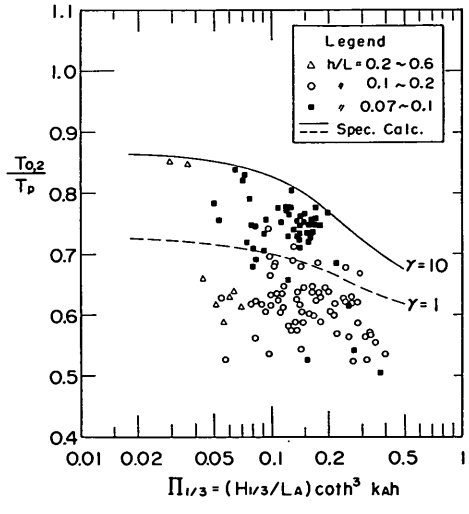


**Fig. 15** Coastal Wave Data of Apparent Decrease of Mean Zero-Upcrossing Period Derived from Wave Spectrum versus Nonlinearity Parameter

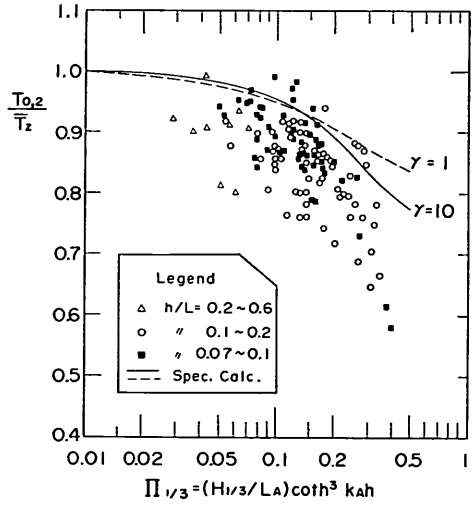


**Fig. 16** Coastal Wave Data of the Ratio of Mean Wave Period Derived from Spectrum to the Mean Period Counted on Wave Record versus Wave Nonlinearity Parameter

### (2) Spectral Peakedness Parameter

The author [1970] has proposed the following parameter to quantitate the sharpness of spectral peak:

$$Q_p = 2\int_0^\infty f S^2(f)\,df \Big/ \left[\int_0^\infty S(f)\,df\right]^2 . \tag{30}$$

This parameter has been found useful in the study of wave grouping [*e.g.*, *Rye* 1982, *Su et al.* 1982, and *Goda* 1983].

The spectral peakedness parameter $Q_p$ is affected by the presence of nonlinear spectral components too. Figure 17 shows the result of numerical calculation of $Q_p$

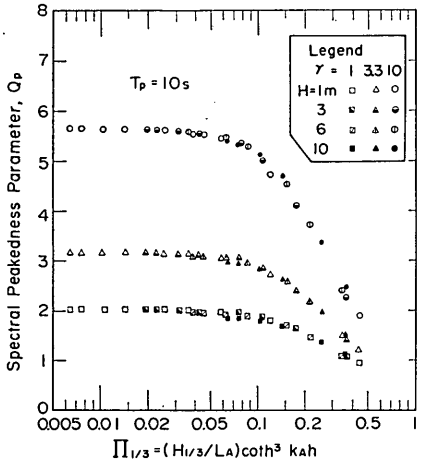


**Fig. 17** Apparent Decrease of Spectral Peakedness Parameter for JONSWAP-type Spectrum in Terms of Wave Nonlinearity Parameter

for the JONSWAP-type spectra with $\gamma=1$, 3.3, and 10 in the range of $H_{1/3}=1$ to 6 m at $T_p=10$ s. Each spectrum experiences a decrease of $Q_p$ value as the wave nonlinear parameter increases. The effect of the input wave height is well expressed with the parameter of $\Pi_{1/3}$. The decrease of $Q_p$ value is mostly due to the apparent increase of the zero-th spectral moment due to the growth of secondary spectral peak. It has been noticed in the analysis of swell records at Caldera Port that the value of $Q_p$ would have been increased by 10 to 30% by setting the upper bound of the integrations of Eq. 30 at $f=1.8f_p$ [*Goda* 1983]. Such a measure would be necessary in the future analysis of wave data on the basis of theoretical calculation of Fig. 17.

### (3) Slope of Wave Spectrum

A characteristic parameter of the shape of wave spectrum is its slope in the range of frequency higher than the peak frequency. Since the paper by *Phillips* [1958], the wave spectrum at the higher frequency range has been fitted with the functional form of $f^{-5}$, though *Toba* [1973] argues better fitness of $f^{-4}$ than $f^{-5}$. In the water of intermediate depth, *Goda and Nagai* [1974] have reported that spectra of coastal waves have the slope of $m\fallingdotseq 4$ in the form of $f^{-m}$ on the average and some spectra show the slope milder than $m=3$.

By examining the slope of spectra of wind waves in laboratory, *Huang et al.* [1981] have proposed a unified two-parameter wave spectral model of the following:

$$S(\omega)=\beta g^2\omega_p^{m-5}\omega^{-m}\exp\left[-\frac{m}{4}\left(\frac{\omega}{\omega_p}\right)^{-4}\right], \tag{31}$$

where

$$\beta=(2\pi\xi)^2\frac{m^{(m-1)/4}}{4^{(m-5)/4}}\cdot\frac{1}{\Gamma[(m-1)/4]}, \tag{32}$$

$$m=\left|\frac{2\log\sqrt{2}\pi\xi}{\log 2}\right|, \tag{33}$$

$$\xi=\frac{\eta_{\rm rms}}{L_p}\fallingdotseq\frac{\pi H_{1/3}}{2gT_{1/3}^2}. \tag{34}$$

The parameter $\xi$ is called the significant slope of the wave field. Huang *et al.* named the above spectral model as the Wallops spectrum.

By converting $\eta_{\rm rms}$ into $H_{1/3}$ with the approximate relation of $H_{1/3}=4\eta_{\rm rms}$ and recovering $T_p$ from $L_p$ with the dispersion relation of $L_p=2\pi g/\omega_p^2$ in deep water, Eqs. 31 and 32 are rewritten as

$$S(f)=\frac{1}{4}\left(\frac{m}{4}\right)^{(m-1)/4}\cdot\frac{1}{\Gamma[(m-1)/4]}H_{1/3}{}^{2}T_{p}(T_{p}f)^{-m}\exp\left[-\frac{m}{4}(T_{p}f)^{-4}\right]. \qquad (35)$$

This is a spectral model specified with three parameters of $H_{1/3}$, $T_p$, and $m$. But the parameter $m$ is uniquely determined by Eqs. 33 and 34 with $H_{1/3}$ and $T_p$, and thus it is a two-parameter spectral model.

In deriving the above spectral model, Huang *et al.* measured the slope of wave spectrum with the straight line (on the logarithmic paper) connecting the main and secondary peaks by taking it as the envelope of spectrum. By adopting this definition, the slope of theoretical spectra with nonlinear secondary interaction components have been measured for a Wallops-type spectrum of Eq. 35. The parameter $m$ was not determined by Eq. 33, but it was given one of several prescribed values. Figure 18 shows the variation of apparent slope $m^*$ with respect to the wave nonlinearity parameter of $\Pi_{1/3}$. Three values of $m$ from 5 to 10 are used for the wave height ranging from $H_{1/3}=1$ to 15 m at $T_p=10$ s. When the value of $\Pi_{1/3}$ is small, the secondary peak does not emerge as seen in the example of calculated spectrum at $h=23.4$ m in Fig. 12. To make the analysis consistent, however, the line was drawn by connecting the main peak and the point of spectral density at the twice peak frequency even if the secondadry peak was not noticeable.

The result shown in Fig. 18 clearly indicates that the apparent slope of wave spectrum is a function of the wave nonlinearity parameter and the original slope parameter, $m$. The effect of wave height is well included in the nonlinearity parameter. Another point of interest is that the asymptotic value of $m^*$ at $\Pi_{1/3}\to 0$ does not agree with the given value of $m$. For example, the spectrum with $m=10$ yields $m^*=6.7$ and the one with $m=5$ yields $m^*=3.3$. The difference is owing to the multiplier function of $\exp[-m(T_pf)^{-4}/4]$ in the right-hand side of Eqs. 31 and 35.

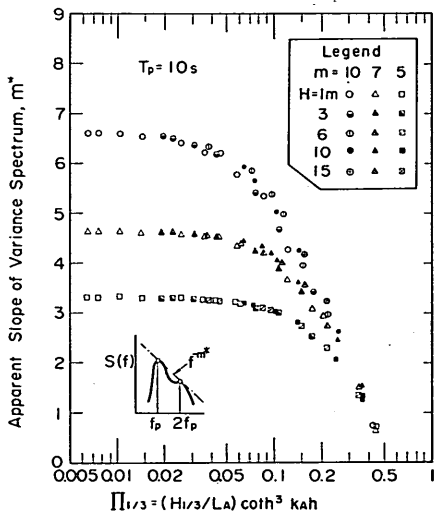


**Fig. 18** Variation of Apparent Slope of Wallops-type Spectrum in Terms of Wave Nonlinearity Parameter

Analysis was also made for the field data by using the same definition of apparent slope. Figure 19 shows the swell data of Caldera Port. The data fit well to the theoretical variation of a Wallops-type spectrum with $m=10$. This is in agreement with the actual slope of wave spectra ranging from 8 to 10, which was determined by fitting a straight line in the frequency range of $f_p<f<1.8f_p$ by means of the least square method. The agreement of swell data with theoretical calculation is somewhat expected, because the apparent slope is an indication of relative magnitude of nonlinear secondary spectral peak to the main peak and the capability of the wave interaction theory to predict the formation of secondary peak has been demonstrated in Fig. 11. The field data at the coastal stations around Japan are shown in Fig. 20. As these data represent various stages of wind waves and young swell, wider scatter of data than

Fig. 19 appears. But the original slope parameter of $m$=5 to 7 fits to the field data as a whole.

The relation between $m$ and $\xi$ in Eq. 33 proposed by *Huang et al.* [1981] is not applicable to the present data of both swell and wind waves, which fundamentally belong to waves in intermediate-depth water. The applicability of Eqs. 33 to wind awaves in deep water in general is questionable too. For it is well known that as the nondimensional fetch of wind waves increases, the wave steepness decreases and the spectral peak becomes flattened. *Mitsuyasu et al.* [1980] have exhibited a decreases of the peak enhancement factor $\gamma$ with the increase of nondimensional fetch. Probably the Wallops spectrum is better employed as a three-parameter spectral model with the value of $m$ so assigned to fit the spectral data best.

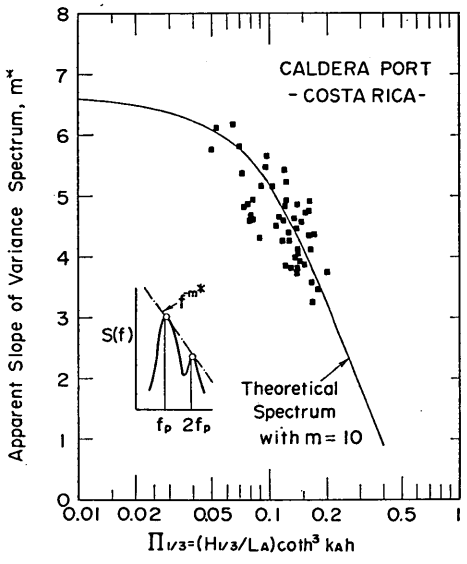


**Fig. 19** Caldera Port Data of Apparent Slope of Observed Wave Spectrum versus Wave Nonlinearity Paramteer

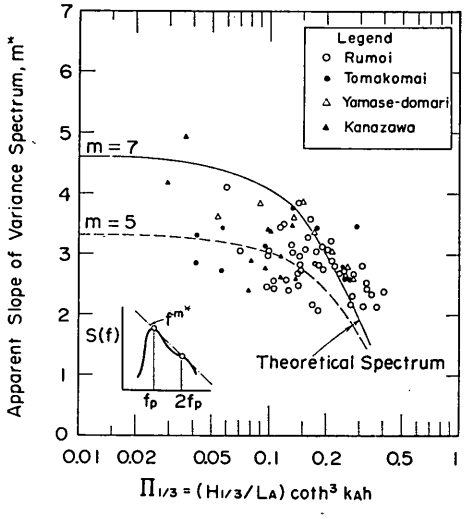


**Fig. 20** Japanese Port Data of Apparent Slope of Observed Wave Spectrum versus Wave Nonlinearity Parameter

### (4) Wave Energy in the Low Frequency Range

The observed spectra of field data shown in Fig. 11 as well as the theoretical calculation of nonlinear spectrum shown in Fig. 12 exhibit the presence of considerable wave energy in the low frequency range. Because such a low frequency energy suggests a formation of surf beats, examination of the wave energy in the range of frequency below $0.5f_p$ was made on theoretical second order wave spectra. Figure 21 shows the ratio of low frequency energy denoted with $m_\zeta$ to the total energy $m_0$. The ratio is shown in its square-root value, so as to indicate a representative height of low frequency components. The JONSWAP-type spectra with $\gamma$=1 and 10 were used in the analysis with $H_{1/3}$ in the range of 1 to 10 m, and the data in the relative water depth not exceeding 0.2 are shown here. Though there exists some influence of absolute magnitude of wave height, the relative height of low frequency components seems to be well represented as a function of the wave nonlinearity parameter of $\Pi_{1/3}$.

The analysis of field data, however, does not support the theoretical prediction. Figure 22 shows the relative height of low frequency components of wave spectra observed at coastal stations. The relative height of field data are scattered in the range of 0.06 to 0.3 without appreciable correlation with the wave nonlinearity parameter. The difference between the theoretical prediction and the field data is partly due to the presence of genuine long-period waves in the sea. Another possible cause is the partial breaking of wave trains in relatively shallow water, to which phenomenon the theory of secondary wave interaction is invalid. In any case, the mechanism of the generation of surf beats itself is not clarified yet. Nonlinear wave interaction is a possible mechanism, but some other mechanisms may be working upon the phenomenon of surf beats as well.

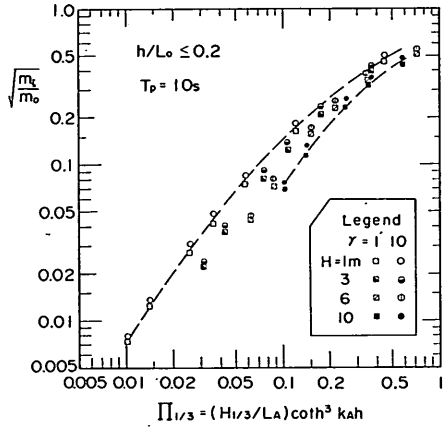


**Fig. 21** Relative Height of Low-Frequency Spectral Components for JONSWAP-type Spectrum in Terms of Wave Nonlinearity Parameter

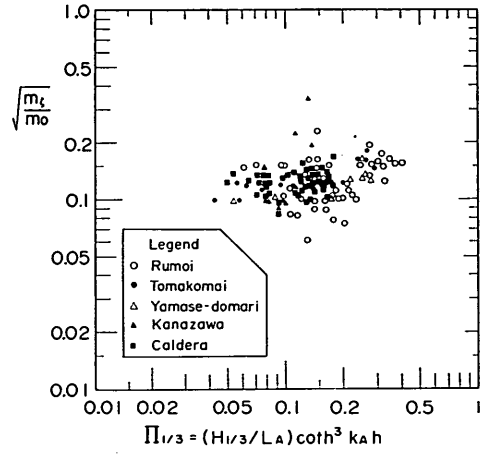


**Fig. 22** Coastal Wave Data of Relative Height of Low-Frequency Components versus Wave Nonlinearity Parameter

## 5. Discussions

The present report takes the stand of linear spectral wave model modified with incorporation of nonlinear interaction components. Swell data of Caldera Port in Costa Rica have been verified to have uniform, quasi-random phases among the spectral components around the main peaks [*Goda* 1983]. Capability of wave interaction theory to explain the nonlinear behaviours of spectral parameters as described in Chapter 4 is a proof that the linear spectral wave model is valid in effect.

As described in Chapter 1, however, various efforts are being made to construct nonlinear models of wind waves. *Sobey and Colman* [1982], for example, propose the use of "Scattering Data" by the Zakharov-Shabat scattering transformation in the analysis and synthesis of weakly nonlinear waves. *Yasuda et al.* [1982] on the other hand is proposing a nonlinear wave model of soliton spectrum in shallow water region by decomposing wave records into a train of cnoidal waves with various heights and periods. Agreements between field data and finite amplitude wave theories in various

nonlinear properties of wave profiles described in Chapter 3 seem to encourage their approach, though the transition from deep water to intermediate-depth waves cannot be handled with the cnoidal wave theory.

From the standpoint of linear spectral wave model, development of higher order theory of wave interactions is desired. *Masuda et al.* [1979] has obtained a formula of tertiary interactions for deepwater waves with directional spectra, while *Hamanaka and Kawasaki* [1980] have calculated the secondary interactions of directional waves in water of finite depth. Extension of tertiary interaction theory into shallow water region should be encouraged.

The presence of nonlinear components in wave spectra distorts several wave parameters derived from spectra. The mean zero-upcrossing period and the spectral peakedness parameter are the examples discussed in Chapter 4. The spectral width parameter of $\varepsilon=[1-m_2^2/(m_0m_4)]^{1/2}$ by *Cartwright and Longuet-Higgins* [1956] and another of $\nu=[m_0m_2/m_1^2-1]^{1/2}$ by *Longuet-Higgins* [1957] are both obscured by the nonlinear spectral components. In fact, the former parameter if calculated with the full frequency range of wave spectrum does not yield any information of spectral bandwidth, but it merely reflects the relative density of data sampling interval in terms of the spectral peak frequency [*Goda* 1974].

In order to remove the influence of nonlinear spectral components, *Nolte and Hsu* [1972] made a truncation of spectra above the frequency of $1.5f_p$ for the study of wave group statistics. *Honda and Mitsuyasu* [1977, 1978] employed a cutoff frequency of $2f_p$ for the examination of statistical properties of wind waves in laboratory and in the ocean. *Nolte and Hsu* [1979] further proposed the use of a lowpass filter with the shutoff frequency of $2f_p$. They demonstrated that by applying the filter to wave data the nonlinearity of wave profiles was diminished and the wave height and period distributions could become in better agreement with statistical theories. Although the author believes that the original wave records are better used to yield the heights and periods of representative waves by the zero-upcrossing method, the procedure of cutting-off the high frequency portion of observed wave spectrum is a simple and convenient method to avoid the contamination by nonlinear spectral components when estimating parameters derived from wave spectrum. The selection of cutoff frequency is better made after resolving the nonlinear components from the observed wave spectrum for several representative cases by the theory of nonlinear wave interactions.

## 6. Conclusions

The present study on the nonlinear behaviours of water waves can be summarized with the following conclusions:

1. Most of nonlinear behaviours of regular waves in laboratory and random waves in the sea can be described as the unique functions of a newly proposed wave nonlinearity parameter $\boldsymbol{\Pi}$.
2. The Stokes waves of third order approximation and cnoidal wave of second order approximation are smoothly connected with the aid of the wave nonlinearity parameter as far as wave profiles are concerned. The applicable range of the former waves is approximately $\boldsymbol{\Pi}=0.2$ or less.
3. As to the properties of wave profiles, the wave nonlinearity parameter governs the ratio of crest elevation to wave height, the skewness, and the ratio of wave height

to the root-mean-square surface elevation in the region of deep to shallow water. The applicability of the wave nonlinearity parameter to the skewness of wind waves in deep water requires further examination, however.

4. Nonlinear wave spectral components have been confirmed to be originated from wave interaction among spectral components. The magnitude of these spectral components is governed by the wave nonlinearity parameter.

5. Among the wave parameters derived from wave spectrum, the wave nonlinearity parameter can describe the degree of distortion of the mean zero-upcrossing period, the spectral peakedness parameter, and the slope of wave spectrum in the high frequency range as the result of nonlinear wave interactions among spectral components. The presently available theory of secondary wave interactions, however, is insufficient in accuracy to predict the effects of wave nonlinearity fully, and a higher order theory is needed.

6. The phenomenon of surf beats cannot be explained with the secondary wave interaction theory alone.

(*Received on June 30, 1983*)

## References


1) ARAE [1982]: *Wave and Wind Directionality: Applications to the Design of Structures*, Proc. Int. Conf., Paris, 1981, Éditions Technip.
2) BENJAMIN, T. B. and FEIR, J. E. [1967]: The disintegration of wavetrains on deep water, *J. Fluid Mech.*, Vol. 27, pp. 417–430.
3) CARTWRIGHT, D. E. and LONGUET-HIGGINS, M. S. [1956]: The statistical distribution of the maxima of a random function, *Proc. Royal Soc. London, Ser. A.*, Vol. 237, pp. 212–232.
4) DEAN, R. G. [1965]: Stream function representation of nonlinear ocean waves, *J. Geophys. Res.*, Vol. 70, No. 18, pp. 4561–4572.
5) GODA, Y. [1964]: Wave forces on a vertical circular cylinder: Experiments and proposed method of wave force computation, *Rept. Port and Harbour Res. Inst.*, No. 8, 74 p.
6) GODA, Y. [1970]: Numerical experiments on wave statistics with spectral simulation, *Rept. Port and Harbour Res. Inst.*, Vol. 9, No. 3, pp. 3–57.
7) GODA, Y. [1974]: Estimation of wave statistics from spectral information, *Proc. Int. Symp. on Ocean Wave Measurement and Analysis*, ASCE, New Orleans, pp. 320–337.
8) GODA, Y. [1977]: *Design of Harbour Structures against Random Seas—Introduction to Ocean Wave Engineering—*, Kajima Pub. Soc., Tokyo, p. 20 (*in Japanese*).
9) GODA, Y. [1979]: A review on statistical interpretation of wave data, *Rept. Port and Harbour Res. Inst.*, Vol. 18, No. 1, pp. 5–32.
10) GODA, Y. [1983]: Analysis of wave grouping and spectra of long-travelled swell, *Rept. Port and Harbour Res. Inst.*, Vol. 22, No. 1, p. 3–41.
11) GODA, Y. and ABE, Y. [1968]: Apparent coefficient of partial reflection of finite amplitude waves, *Rept. Port and Harbour Res. Inst.*, Vol. 7, No. 3, pp. 3–58.
12) GODA, Y. and NAGAI, K. [1974]: Investigation of the statistical properties of sea waves with field and simulation data, *Rept. Port and Harbour Res. Inst.*, Vol. 13, No. 1, pp. 3–37 (*in Japanese*).
13) HAMADA, T. [1965]: The secondary interactions of surface waves, *Rept. Port and Harbour Res. Inst.*, No. 10, 28 p.

14) HAMANAKA, K. and KAWASAKI, K. [1980]: Asymptotic solution of random gravity waves in shallow water, *Proc. 27th Japanese Conf. Coastal Eng.*, pp. 16–19 (*in Japanese*).
15) HONDA, T. and MITSUYASU, H. [1977]: On the joint distribution of the heights and periods of wind-generated waves, *Proc. 24th Japanese Conf. Coastal Eng.*, pp. 83–87 (*in Japanese*).
16) HONDA, T. and MITSUYASU, H. [1978]: On the joint distribution of the heights and periods of ocean waves, *Proc. 25th Japanese Conf. Coastal Eng.*, pp. 75–79 (*in Japanese*).
17) HORIKAWA, K. and NISHIMURA, H. [1976]: A comparative study on Stokes waves and cnoidal waves, *Proc. 23rd Japanese Conf. Coastal Eng.*, pp. 371–375 (*in Japanese*).
18) HUANG, N. E. and LONG, S. R. [1980]: An experimental study of the surface elevation probability distribution and statistics of wind-generated waves, *J. Fluid Mech.*, Vol. 101, pp. 179–200.
19) HUANG, N. E., LONG, S. R., TUNG, C-C., YUEN, Y., and BILVEN, L. F. [1981]: A unified two-parameter wave spectral model for a generous sea state, *J. Fluid Mech.*, Vol. 112, pp. 203–224.
20) IWAGAKI, Y. [1964]: Studies on cnoidal waves (First report)—on the wave steepness and profile-, *Disaster Prevention Res. Inst. Annuals*, No. 7, Kyoto Univ., pp. 373–386 (in Japanese).
21) LAITONE, E. V. [1960]: The second approximation to cnoidal and solitary waves, *J. Fluid Mech.*, Vol. 9, pp. 430–444.
22) LAKE, B. M. and YUEN, H. C. [1978]: A new model for nonlinear wind waves. Part 1. Physical model and experimental evidence, *J. Fluid Mech.*, Vol. 88, pp. 33–62.
23) LONGUET-HIGGINS, M. S. [1957]: The statistical analysis of a random, moving surface, *Phil. Trans. Roy. Soc. London, Ser. A* (966), Vol. 249, pp. 321–387.
24) LONGUET-HIGGINS, M. S. [1975]: Integral properties of periodic gravity waves of finite amplitude, *Proc. Roy. Soc. London, Ser. A.*, Vol. 342, pp. 157–174.
25) LONGUET-HIGGINS, M. S. [1980]: On the distribution of the heights of sea waves: Some effects of nonlinearity and finite band width, *J. Geophys. Res.*, Vol. 85, No. C3, pp. 1519–1523.
26) MCCLAIN, C. R., CHEN, D. T. and HART, W. D. [1982]: On the use of laser profilometry for ocean wave studies, *J. Geophys. Res.*, Vol. 87, No. C12, pp. 9509–9515.
27) MASUDA, A., KUO, Y. Y., and MITSUYASU, H. [1979]: On the dispersion relation of random gravity waves. Part 1. Theoretical framework, *J. Fluid Mech.*, Vol. 92, pp. 717–730.
28) MERVILLE, W. K. [1982]: The instability and breaking of deep-water waves, *J. Fluid Mech.*, Vol. 115, pp. 165–185.
29) MITSUYASU, H., TASAI, F., SUHARA, T., MIZUUO, S., OHKUSU, M., HONDA, T. and RIKIISHI, K. [1980]: Observation of the power spectrum of ocean waves using a clover buoy, *J. Physical Oceanography*, Vol. 10, No. 2, pp. 286–296.
30) MOLLO-CHRISTENSEN, E. and RAMAMONJIARISOA, A. [1978]: Modeling the presence of wave groups in a random wave field, *J. Geophys. Res.*, Vol. 83, No. C8, pp. 4117–4122.
31) NOLTE, K. G. and HSU, F. H. [1972]: Statistics of ocean wave groups, *Prepr. 4th Offshore Tech. Conf.*, OTC 1688.
32) NOLTE, K. G. and HSU, F. H. [1979]: Statistics of larger waves in a sea state, *Proc. ASCE*, Vol. 105, No. WW4, pp. 389–404.
33) PHILLIPS, O. M. [1958]: The equilibrium range in the spectrum of wind-generated waves, *J. Fluid Mech.*, Vol. 4, pp. 426–434.
34) RICE, S. O. [1944]: Mathematical analysis of random noise, reprinted in *Selected Papers on Noise and Stochastic Processes*, Dover Pub., Inc., 1954, pp. 133–294.

35) RYE, H. [1982]: Ocean wave groups, *Dept. Marine Tech., Norwegian Inst. Technology*, Rept. UR-82–18, 214 p.
36) SHUTO, N. [1974]: Nonlinear long waves in a channel of variable section, *Coastal Engg. in Japan*, JSCE, Vol. 17, pp. 1–12.
37) SKJELBREIA, L. and HENDRICKSON, J. [1960]: Fifth order gravity wave theory, *Proc. 7th Conf. Coastal Eng.*, Hague, pp. 184–196.
38) SOBEY, R. J. and COLMAN, E. J. [1982]: Natural wave trains and scattering transform, *Proc. ASCE* Vol. 108, No. WW3, pp. 272–290.
39) STOKES, G. G. [1847]: On the theory of oscillatory waves, *Trans. Cambridge Philosoph. Soc.*, Vol. 8.
40) SU, M–Y. [1982]: Evolution of groups of gravity waves with moderate to high steepness, *Phys. Eluids*, Vol. 25, No. 12, pp. 2167–2174.
41) SU, M-Y., BERGIN, M. Y., and BALES, S. L. [1982]: Characteristics of wave groups in storm seas, *Proc. Ocean Structural Dynamics Symp. '82*, Oregon State Univ., Corvallis, Oregon.
42) TICK, L. J. [1963]: Nonlinear probability models of ocean waves, *Ocean Wave Spectra*, Prentice Hall, Inc., pp. 163–169.
43) TOBA, Y. [1973]: Local balance in the air-sea boundary processes, III. On the spectrum of wind waves, *J. Oceanogr. Soc. Japan*, Vol. 29, pp. 209–220.
44) URSELL, F. [1953]: The long-wave paradox in the theory of gravity waves, *Proc. Cambridge Philosph .Soc.*, Vol. 49, pp. 685–694.
45) WIEGEL, R. L. (ed.) [1982]: *Proc. Conf. Directional Wave Spectra Applications*, Berkeley, 1981, ASCE, 495 p.
46) YASUDA, T. SHINODA, S., and TSUCHIYA, Y. [1982]: Dynamic expression of waves in shallow water by the theory of soliton spectra, *Proc. 29th Japanese Conf. Coastal Eng.*, pp. 36–40 (*in Japanese*).

## Appendix: List of Symbols

| | | |
|---|---|---|
| $C$ | : | wave celerity |
| $f$ | : | frequency |
| $f_p$ | : | frequency at spectral peak |
| $g$ | : | acceleration of gravity |
| $h$ | : | water depth |
| $h_t$ | : | water depth measured from wave trough |
| $H$ | : | wave height in general |
| $H_{max}$ | : | height of the highest zero-upcrossing wave in a wave record |
| $H_{1/3}$ | : | significant wave height or the mean of the heights of highest one-third zero-upcrossing waves |
| $k$ | : | wave number ($=2\pi/L$) |
| $k_A$ | : | wave number calculated by the small amplitude wave theory (Eq. 2) |
| $L$ | : | wavelength in general |
| $L_A$ | : | wavelength calculated by the small amplitude wave theory (Eq. 2) |
| $L_p$ | : | wavelength corresponding to the frequency at spectral peak |
| $m$ | : | slope parameter of Wallops type spectrum (cf. Eq. 35) |
| $m^*$ | : | apparent slope of high frequency side of wave spectrum |
| $m_n$ | : | n-th moment of wave spectrum (Eq. 29) |
| $m_\zeta$ | : | energy of low frequency components of wave spectrum |
| $Q_p$ | : | spectral peakedness parameter (Eq. 30) |
| $S(f)$ | : | wave spectrum or variance spectral density function of surface elevation |

$T$ : wave period in general
$T_{max}$ : period of the highest zero-upcrossing wave in a wave record
$\bar{T}_z$ : mean of zero-upcrossing wave periods counted on a wave record
$T_{1/3}$ : significant wave period or the mean of the periods of highest one-third zero-upcrossing waves
$T_{0,2}$ : mean wave period defined with wave spectrum by Eq. 28
$T_p$ : wave period corresponding to the frequency at spectral peak

$\sqrt{\beta_1}$ : skewness of surface elevation
$\gamma$ : peak enhancement factor of JONSWAP spectrum (cf. Eq. 25)
$\varepsilon$ : perturbation parameter related with wave steepness (Eq. 9)
$\eta$ : surface elevation above the mean water level
$\eta_c$ : elevation of wave crest above the mean water level
$\eta_{max}$ : elevation of highest wave crest in a wave record
$\eta_{rms}$ : root-mean-square value of surface elevation
$\kappa$ : modulus of elliptic function
$\Pi$ : wave nonlinearity parameter defined by Eq. 1
$\Pi_{max}$ : wave nonlinearity parameter corresponding to the highest wave
$\Pi_{1/3}$ : wave nonlinearity parameter corresponding to significant wave
$\omega$ : angular frequency ($=2\pi f$)